CrossMark

Printed Monopole Antenna for Ultra-Wideband Application with Tunable Triple Band-Notched Characteristics

Manas Sarkar[1] · Santanu Dwari[1] · Anitha Daniel[2]

Abstract In this paper, a compact ultra-wideband (UWB) microstrip-fed printed monopole antenna with triple band-notched characteristics is proposed. The proposed design consists of a radiating patch with two bevels at the bottom edge and the modified ground plane with two bevels of its upper edge to cause the wideband from 3.1 to 10.6 GHz for UWB application. Additionally, a triangular cut is introduced at the upper edge of the ground plane for improving the impedance matching beyond 6 GHz. The band notch at 3.4 GHz is achieved with a pair of slots along patch length and placed symmetrically on both the sides of the patch whereas notch band at 5.2 GHz is achieved using complementary split ring resonator (CSRR) on the patch. The third notch frequency at 5.8 GHz also achieved by using a pair of CSRR on the ground plane. The antenna size is 24 mm × 34.6 mm and designed using FR4 substrate having $\varepsilon_r = 4.4$ and thickness of 0.8 mm. Design and optimizations have been carried out using HFSS v13.0 and there is good agreement with measured results. The proposed antenna exhibits a nearly omnidirectional radiation pattern in the H-plane, and a dipole-like radiation pattern in the E-plane for the entire pass band.

Keywords Tunable triple band notched · Ultra-wideband (UWB) · Printed monopole antenna · Complementary split ring resonator (CSRR)

✉ Manas Sarkar
   mns_sarcar@yahoo.com

[1] Department of Electronics Engineering, Indian School of Mines, Dhanbad 826004, Jharkhand, India

[2] Radar Development Area, ISTRAC/ISRO, A1-6, Peenya Industrial Estate, Bangalore 560058, Karnataka, India

1 Introduction

Research on ultra-wideband (UWB) has increased considerably since Federal Communication Commission (FCC) had allocated the frequency range from 3.1 to 10.6 GHz for commercial use of high data rate wireless communication [1]. As an essential part of ultra-wideband (UWB) system, UWB antennas have drawn wide interest for researchers. Recently, due to many attractive features like low profile, light weight and low cost printed monopole antennas are frequently used for UWB application. These antennas should have a broad impedance bandwidth of 3.1–10.6 GHz, stability in radiation characteristics with good omni-directional pattern and compact in size. Additionally some frequency bands including World Interoperability for Microwave Access (WiMAX) system at 3.5 GHz (3.4–3.69 GHz), Wireless Local Area Network (WLAN) at 5.2 GHz (5.15–5.35 GHz), and 5.8 GHz (5.725–5.825 GHz) have been allocated within the designated ultra-wideband. To avoid electromagnetic interference from those narrowband communication systems, band rejection filters can be used at the RF front-end of the UWB systems. This gives rise to system complication with increase in size and cost, as well as an increase of insertion loss. To avoid those problems, the UWB antennas are required to feature with the band-notched property.

Ultra-wideband characteristics of printed monopole antennas can be achieved in many ways like using electromagnetic band gap (EBG) structure, open slot or using Sierpinski fractals [2–4]. In recent years different techniques to suppress some specific narrow bands of UWB monopole antenna have been reported. The commonly used techniques are cutting resonant slots on patch, feed line or on ground plane [5–9] or using stub [10–12], defective ground structure [8, 10, 13] or introducing ring or loop resonators [14, 15]. Using the above

Fig. 1 Geometry of the proposed antenna **a** dimension details, all dimensions are in mm; L1 = 12.8 mm, r1 = 1.85 mm and r2 = 3.6; photograph of **b** top and **c** bottom view of fabricated antenna

techniques single [6, 7], dual [5, 8, 10–12, 14] and triple [9, 13, 15–17] band notched antennas are reported. However UWB antennas with multiple band rejection frequencies have two major limitations namely, mutual coupling and the other one is larger antenna size.

Those two major drawbacks are overcome by using complementary split ring resonator (CSRR) to get band notched characteristics. In this paper a microstrip-fed compact planar monopole antenna is presented for UWB application with three band notched characteristics centered at 3.4 GHz, along with two very closely spaced at 5.2 and 5.8 GHz. The lower notch frequency at 3.4 GHz is achieved using two symmetrical slots on the patch whereas the higher notch frequency at 5.2 GHz is achieved using complementary split ring resonator (CSRR) at the centre of the patch. A pair of rectangular CSRR is used symmetrically at both the sides of the ground plane to achieve the third notched frequency at 5.8 GHz. In addition to the bevels respectively at the lower and upper edge of the patch and ground plane, a triangular cut has been introduced at the upper edge of the ground for the impedance matching beyond 6 GHz.

Organization of this paper is as follows. Section 2 presents the configuration of the proposed antenna. The proposed antenna was fabricated and the measured results are produced in Sect. 3 and compared with the simulated results. Further scope and conclusion is detailed in Sect. 4.

2 Antenna Configuration

The geometry of the proposed printed monopole antenna is shown in Fig. 1. The antenna is fabricated on a low cost FR4 substrate of size 24 mm × 34.6 mm, dielectric constant 4.4, thickness of 0.8 mm and loss tangent 0.02. The bottom of radiating patch has two bevels [18] of height 8 mm and length 10 mm. Also upper side of the ground plane has two bevels of height 3.7 mm and length 7 mm to cover the ultrawide band from 3.1 to 10.6 GHz. The patch is fed with a microstrip line of width 1.5 mm to achieve 50 Ω characteristics impedance. Additionally, a triangular notch of length 6 mm and depth 2 mm is introduced at the upper side of the ground. This results a smooth transition from one resonant mode to another, ensuring good impedance match over a broad band at the higher frequency range.

Since the slots of similar shape of the patch antenna generate stronger resonance than any other slot shape, the rectangular shape slots having one shorted end, and another open end at both the sides of the patch are used to achieve the lower notch frequency at 3.4 GHz. Length of the slot is about a quarter of guided wavelength [18].

Thus slot length can be mathematically expressed as

$$L_g = \frac{\lambda_g}{4} = \frac{c}{4f\sqrt{\varepsilon_{reff}}} \tag{1}$$

where the effective dielectric constant ε_{reff} can be written as

$$\varepsilon_{reff} = (\varepsilon_r + 1)/2 \tag{2}$$

These two slots are parallel to the patch side arm of length 12.8 mm and width 0.5 mm as shown in Fig. 1.

The higher notch frequency at 5.2 GHz is achieved by using complementary split ring resonator (CSRR) at 3.5 mm offset from the centre of the patch. The split ring resonator (SRR) is the two concentric metallic rings having split on opposite side. The complementary split ring resonator (CSRR) is the negative image of SRR and used here as the slot

on the patch to generate the notch frequency at 5.2 GHz. Both the rings of 300° subtended angle are having the radius of 1.85 and 3.6 mm with the slot width of 0.8 mm each. Such a CSRR as shown in Fig. 2a, can be modeled as a LC resonator with an equivalent circuit as shown in Fig. 2b [20]. In this CSRR model, C_c is the capacitance of the disc of radius $r_{ext} - 3y/2 - x/2$ surrounded by outside metal plane at a distance y from the periphery. L_c, parallel combination of the two inductances $L_0/2$ is the inductor connecting the inner disc to the outer metal. Where $L_0 = 2\pi r_0 L_{pul}$ and L_{pul} is the per unit length inductance of the CPWs connecting the inner disc to the outside metal and r_0 is the average radius. The resonance frequency of CSRR is according to the following relation.

$$f_0 = \frac{1}{2\pi\sqrt{L_c C_c}} \tag{3}$$

The third notch frequency at 5.8 GHz is achieved using a pair of complementary split ring resonator (CSRR) of rectangular shape on the ground plane as shown in Fig. 1.

CSRR loaded with microstrip line is shown in Fig. 2c. The equivalent circuit diagram for a CSRR loaded mcrostrip line is shown in the Fig. 2d [21]. Here L is the line inductance and C_p is the coupling capacitance between line and the CSRR. CSRR can be described by means of a parallel tank C_c and L_c being reactive element and loss resistance R which can be neglected for a lossless case. From this model, a frequency for which transmission is zero can be determined from the following relation,

$$f_z = \frac{1}{2\pi\sqrt{L_c(C + C_c)}} \tag{4}$$

(a)   **(b)**

(c)   **(d)**
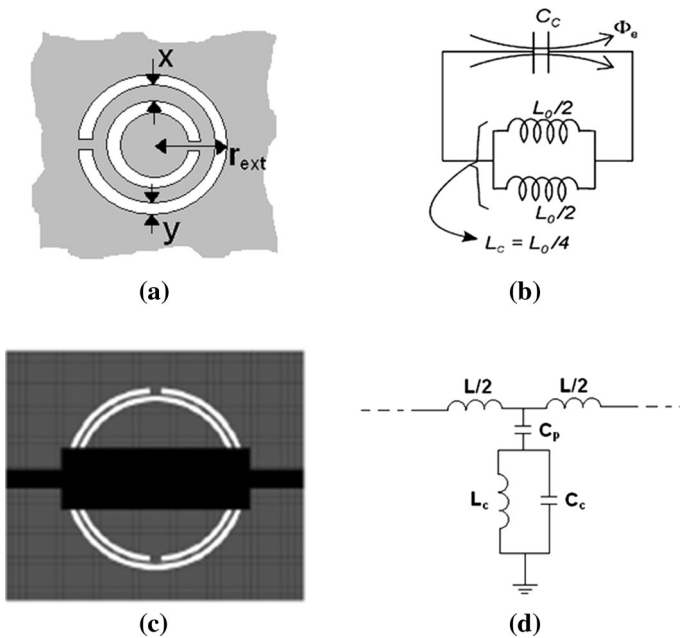
Fig. 2 Topologies for CSRR **a** CSRR model, **b** equivalent circuit, **c** CSRR loaded with microstrip line, **d** equivalent circuit
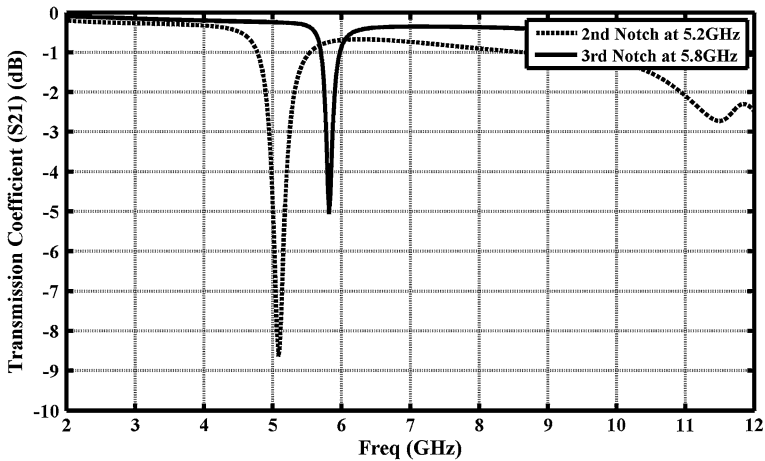
Fig. 3 Frequency responses of CSRR used for 2nd and 3rd notch frequencies

and this frequency can be accurately obtained either by simulation or measurement. Also the frequency at which shunt admittance becomes zero (f_0) is resonance frequency of the parallel resonant circuit and follows Eq. (3). At this frequency, S_{11} curve when plotted on Smith chart, intersects the unit normalized resistance circle. And the inductance L can be found directly. To determine all element values one more relation is required in addition to expressions (3) and (4) which is given below:

$$Z_s\left(j\omega_{\pi/2}\right) = -Z_p\left(j\omega_{\pi/2}\right) \tag{5}$$

where $Z_s(j\omega)$ and $Z_p(j\omega)$ are the series and shunt impedance of the T-circuit model shown in Fig. 2d and $\omega_{\pi/2}$ is the angular frequency at which phase of the transmission coefficient $\phi(S_{21}) = \pi/2$.

Using the relation (3), (4) and (5) the electrical parameters for the CSRR on the patch and ground plane can be calculated. The simulated frequency response curves for these CSRRs are shown in the Fig. 3.

Since the geometry of slot for the first notch at 3.4 GHz is rectangular whereas the slot geometry for the second notch at 5.2 GHz is a CSRR of circular shape, the mutual coupling between those two frequencies is reduced. Also a pair of CSRR of rectangular shape for the third notch frequency at 5.8 GHz is placed at the ground plane. Thus mutual coupling between closely spaced second and third notch is reduced and all the three notch frequencies can be tuned independently.

3 Results and Discussions

The proposed antenna is designed using HFSS v13.0 and parametric optimizations are performed to achieve the final physical dimensions for ultra wide band application as shown in Fig. 1.

Bandwidth of the monopole antenna has been increased using triangular cut at the bottom side of the patch. Further improvement of the bandwidth is achieved using two

bevel sat the top side of the ground plane. This improves the performance at the higher frequency and the operating frequency extends from 3.1 GHz to beyond 10.6 GHz with return loss better than −10 dB.

The first notch frequency corresponding to WiMAX system at 3.4 GHz is achieved by introducing two rectangular slots along patch length and placed symmetrically on both the sides of the patch. These slots behave like slot lines. When their lengths become quarter of their guided wavelength at any frequency, they behave like resonant slot lines. At this frequency, energy mostly concentrates around the slots and resonant radiating modes are disturbed. As a result, notch band appears. Parametric analysis for the slot length (L_1) has been carried out and the length of the slot is optimized as 12.8 mm. The slot width is optimized and maintained as 0.5 mm. The analysis results are shown in the Fig. 4.

The second notch frequency corresponding to WLAN application at 5.2 GHz is achieved by using CSRR of circular shape on the patch. When CSRR is used on radiating patch of UWB antenna, the rejected frequency is forced to be the resonance frequency of the corresponding CSRR and is related to the inductance per unit length between the ring slots, total capacitance of the CSRR and the average radius of the ring [19]. At this frequency, energy mostly concentrates around this CSRR and resonant radiating modes are disturbed. As a result, notch band appears.

Parametric variation of the second notch frequency is shown in Figs. 5 and 6 where notch frequency decreases with the increase of slot length either by radius of ring as shown in Fig. 5 or by increasing the subtended angle as shown in Fig. 6. Radius and subtended angle of both the rings can be varied to optimize the performance of a desired notch frequency. It is to be observed from Figs. 5 and 6 that second notch can be tuned independently without affecting the first notch frequency. The radii r_1 and r_2 of the rings are optimized as 1.85 and 3.6 mm respectively maintaining a subtended angle of 300° for both the rings. Width of the slots are maintained its optimum value as 0.8 mm.

To get the third notch frequency a pair of rectangular CSRR is introduced at the ground placed symmetrically both the sides of the feed line. CSRR loaded with microstrip line is shown in Fig. 2c. The equivalent circuit diagram for a CSRR loaded microstrip line is
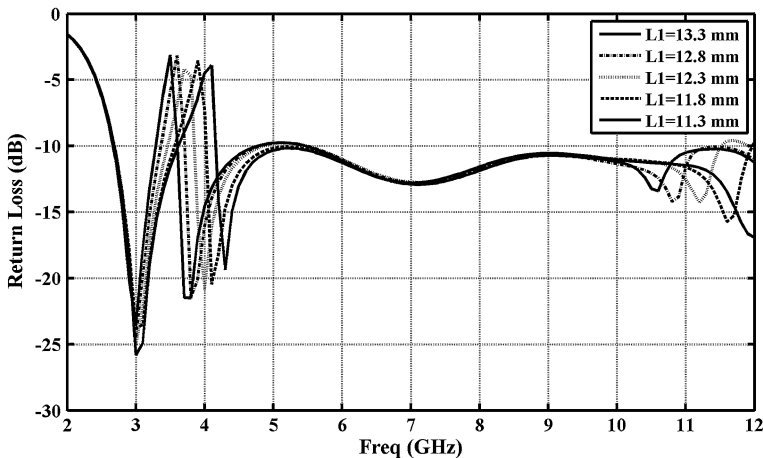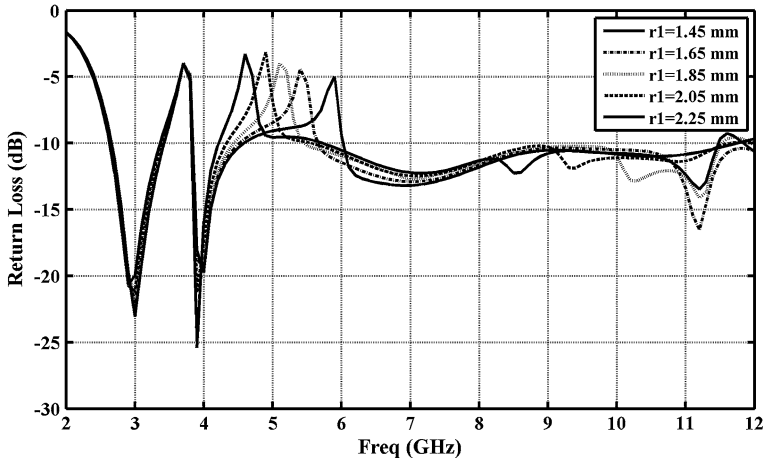

Fig. 4 Optimization of the 1st notch frequency

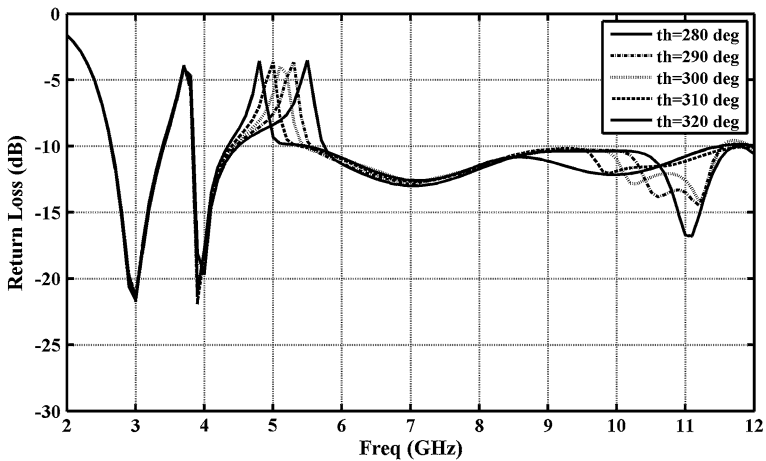**Fig. 5** Optimization of the 2nd notch frequency with radius of ring

Fig. 6 Optimization of the 2nd notch frequency with subtended angle of ring

shown in the Fig. 2d. At the frequency f_z as given in Eq. 4, the shunt path of Fig. 2d would be shorted and no power will reach to the radiating patch. As a result notch band appears.

Figure 7 shows the parametric variation of the outer most rectangular ring length 'a' and height 'b' maintaining separation between larger and smaller rings as 0.7 mm and width of each ring as 0.5 mm. The dimensions 'a' and 'b' are optimized as 4.55 and 5.24 mm to resonate at 5.8 GHz. It can be observed from Fig. 7 that with the increase of total length of ring, resonant frequency decreases while first and second resonant frequency remains unaffected. Also the impedance matching is poor at higher frequency, specially immediately after the third notch frequency. To improve the impedance matching, a triangular notch is introduced at the upper edge of the ground plane. The improvement of return loss performance is easily seen in the Fig. 8, where return loss is compared with different notch depth relative to the performance of that without any notch. It is also seen from Fig. 8 that
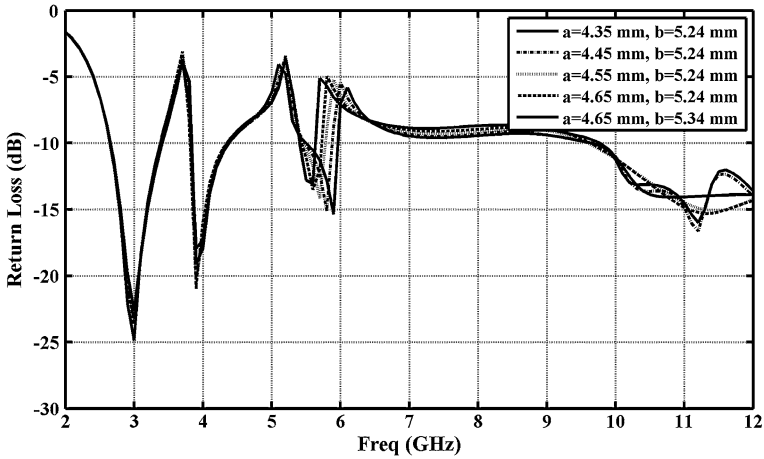
Fig. 7 Optimization of the 3rd notch frequency using dimension of CSRR
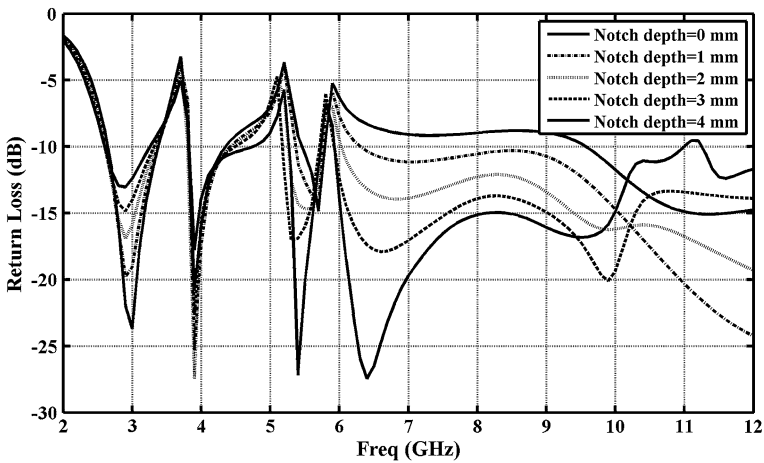

Fig. 8 Optimization of the 3rd notch frequency using triangular cut

the first and the second notch frequency is unaffected by the CSRR at the ground and also due to the triangular cut. This ensures minimum mutual coupling among all three notch frequencies and they can be tuned independently. The final optimized configuration with triple notch band is as shown in Fig. 1a and the fabricated antenna is shown in the Fig. 1b, c. The return loss performance is measured using Agilent N5242A vector network analyzer and compared with the simulated results as shown in the Fig. 9. This shows good agreement between simulated and measured results. The discrepancy is mainly due to measurement environment and fabrication tolerances.

To see the effects of the slots in generating the notched bands, the surface current distribution on the radiating patch and the ground plane of the antenna at three different frequencies are shown in Fig. 10. At the first notched band of frequency 3.4 GHz, the strong distribution of surface current is seen at the edges of larger slots on the patch as
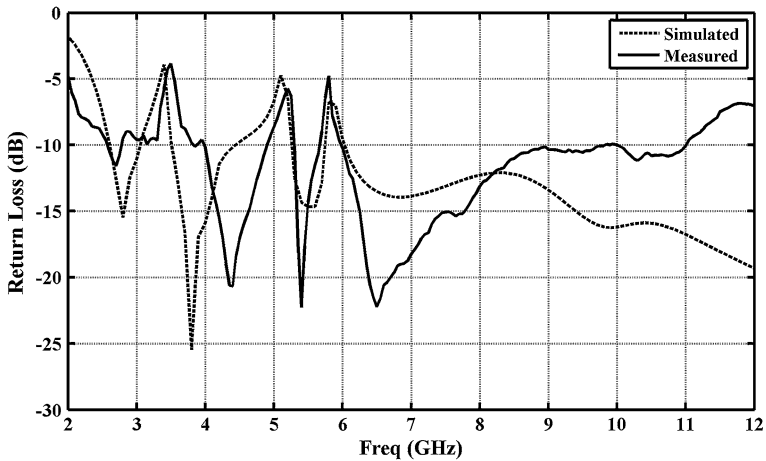
Fig. 9 Comparison of return loss performance of fabricated antenna of triple notch frequency with simulated result
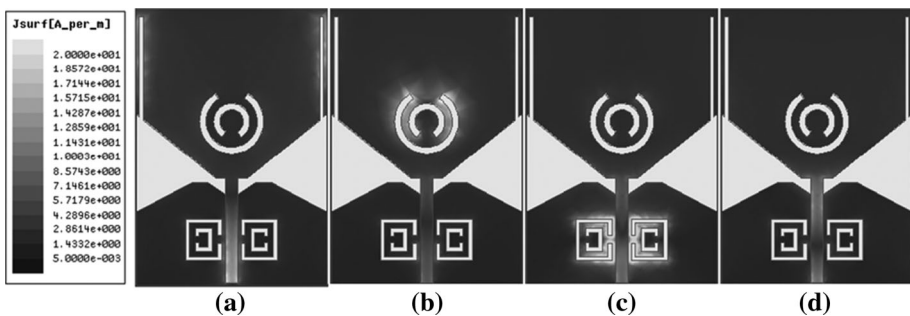

Fig. 10 Surface current distribution on the patch and ground plane at **a** first notch frequency at 3.4 GHz, **b** second notch frequency at 5.2 GHz, **c** third notch frequency at 5.8 GHz and **d** a pass band at 7.5 GHz

shown in the Fig. 10a. Similarly the strong surface current distribution for the second and third notched frequency at 5.2 and 5.8 GHz are seen near the circular CSRR on the patch and rectangular CSRR on the ground as shown in Figs. 8c and 10b respectively. Whereas in the pass band at 7.5 GHz, the surface current distribution is uniform and shown in Fig. 10d.

It is observed from the measured results that the designed monopole antenna covers entire UWB frequency 3.1–11 GHz with triple band notched characteristics centred of 3.4–3.6, 5.1–5.3 and 5.7–5.9 GHz. Moreover the notched frequencies can be adjusted independently by optimization of corresponding slot parameters.

Figure 11 shows the measured radiation pattern of the antenna at 3, 6 and 9 GHz. In xz-plane (H-plane) the pattern is close to omni-directional where as in the yz-plane (E-plane) the pattern is similar to typical dipole antenna. Gain of the realized antenna is measured and plotted along with simulated result in the Fig. 12. It shows that gain is almost flat over the ultra wide band whereas gain decreases drastically at the notch frequencies as expected.
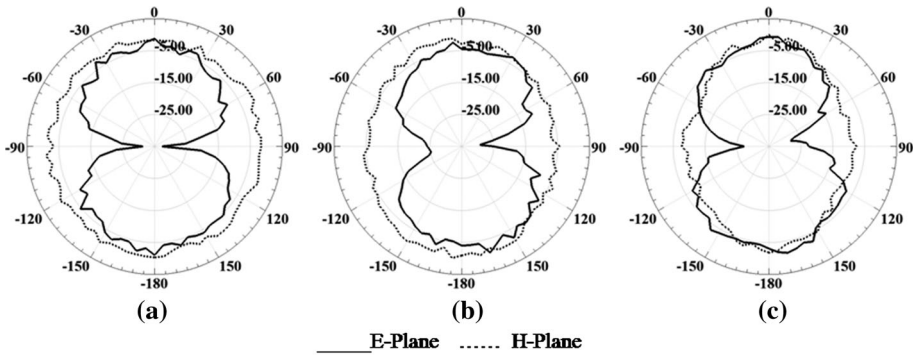
Fig. 11 E and H plane measured radiation pattern at **a** 3 GHz, **b** 6 GHz and **c** 9 GHz
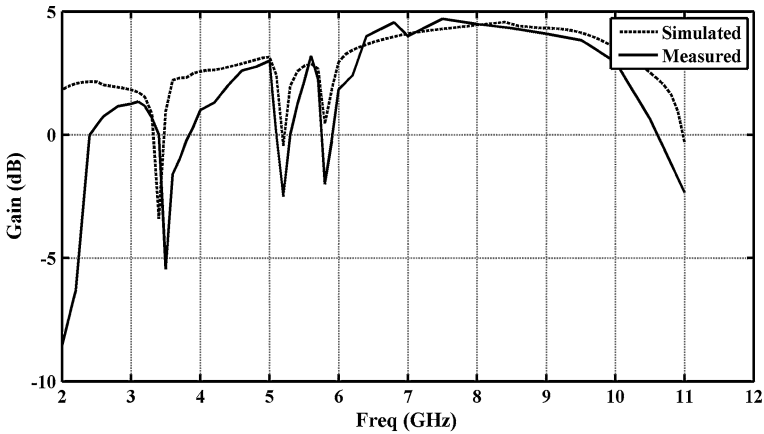

Fig. 12 Gain variation over the ultra-wide band

4 Conclusion

A novel compact printed monopole antenna with triple band notched characteristics for UWB application is investigated. The ultra wide bandwidth is achieved using a planar monopole antenna with triangular shape at the bottom edge of patch and two bevels on the top of ground plane. The triple band notched characteristics is achieved using resonant slot on the patch and CSRR on the patch and ground plane. Two closely spaced notched frequencies are achieved using CSRR of circular and rectangular geometry. The performance degradation beyond 6 GHz, due to CSRR on the ground plane for third notch frequency is compensated by introducing a triangular notch of optimized width and depth on the upper edge of the ground. Mutual coupling among all the notched frequencies are reduced and all three frequencies can be tuned independently by optimizing slot and CSRR parameters. The proposed antenna is fabricated on low cost FR4 and the measured results agree well with simulated one. The radiation pattern of the antenna shows good omni-

directional throughout the UWB range in H plane. Also the proposed antenna gain is flat almost over the operational frequency except at the notched frequencies.

References

1. Federal Communications Commission. *First report and order. Revision of part 15 of the commission's rules regarding ultra-wideband transmission systems*, Feb 2002.
2. Elsheakh, D. N., Elsadek, H. A., Abdallah, E. A., Elhenawy, H., & Iskander, M. F. (2009). Enhancement of microstrip monopole antenna bandwidth by using EBG structures. *IEEE Antennas Wireless Propagation Letters, 8*, 959–962.
3. Song, K., Yin, Y.-Z., Fan, S.-T., Wang, Y.-Z., & Zhang, L. (2009). Open L-slot antenna with rotated rectangular patch for bandwidth enhancement. *Electronics Letters, 45*(25), 1286–1288.
4. Oraizi, H., & Hedayati, S. (2011). Miniaturized UWB monopole microstrip antenna design by the combination of Giusepe Peano and Sierpinski Carpet fractals. *IEEE Antennas and Wireless Propagation Letters, 10*, 67–70.
5. Sarkar, M., Dwari, S., & Daniel, A. (2013). Compact printed monopole antenna for ultra-wideband application with dual band-notched characteristics. *Microwave and Optical Technology Letters, 55*(11), 2595–2600.
6. Zhang, K., Li, Y., & Lang, Y. (2010). Band-notched UWB printed monopole antenna with a novel segmented circular patch. *IEEE Antennas and Wireless Propagation Letters, 9*, 1209–1212.
7. Jang, J.-W., & Hwang, H.-Y. (2009). An improved band rejection UWB antenna with resonant patches and a slot. *IEEE Antennas and Wireless Propagation Letters, 8*, 299–302.
8. Luo, L., Cui, Z., Xiong, J.-P., Zhang, X.-M., & Jiao, Y.-C. (2008). Compact printed ultra-wideband monopole antenna with dual band-notch characteristic. *Electronics Letters, 44*(19), 1106–1107.
9. Trang, N. D., Lee, D. H., & Park, H. C. (2008). Compact printed CPW-fed monopole ultra-wideband antenna with triple subband notched characteristics. *Electronics Letters, 46*(17), 1177–1179.
10. Abdvllahvand, M., Dadashzadeh, G., & Mostafa, D. (2010). Compact dual band-notched printed monopole antennafor UWB application. *IEEE Antennas and Wireless Propagation Letters, 9*, 1148–1151.
11. Hong, C.-Y., Ling, C.-W., Tarn, I.-Y., & Chung, S.-J. (2007). Design of a planar ultrawideband antenna with a new band-notch structure. *IEEE Transactions on Antennas and Propagation, 55*, 3391–3397.
12. Li, Y. S., Yang, X. D., Liu, C. Y., & Jiang, T. (2010). Compact CPW-fed ultra-wideband antenna with band-notched characteristic. *Electronics Letters, 46*(23), 1533–1534.
13. Deng, J. Y., Yin, Y. Z., Zhou, S. G., & Liu, Q. Z. (2008). Compact ultrawideband antenna with tri-band notched characteristic. *Electronics Letters, 44*(21), 1231–1233.
14. Li, W. T., Hei, Y. Q., Feng, W., & Shi, X. W. (2012). Planar antenna for 3G/Bluetooth/WiMAX and UWB applications with dual band-notched characteristics. *IEEE Antennas and Wireless Propagation Letters, 11*, 61–64.
15. Lin, C.-C., Jin, P., & Ziolkowski, R. W. (2012). Single, dual and tri-band-notched ultrawideband (UWB) antennas using capacitively loaded loop (CLL) resonators. *IEEE Transactions on Antennas and Propagation, 60*, 102–109.
16. Trang, N. D., Lee, D. H., & Park, H. C. (2011). Design and analysis of compact printed triple band-notched UWB antenna. *IEEE Antennas and Wireless Propagation Letters, 10*, 403–406.
17. Wong, K. L., Chi, Y. W., Su, C. M., & Chang, F. S. (2005). Band-notched ultra-wideband circular-disk monopole antenna with an arc-shaped slot. *Microwave and Optical Technology Letters, 45*(3), 188–191.
18. Nguyen, D. T., Lee, D. H., & Park, H. C. (2012). Very compact printed triple band-notched UWB antenna with quarter-wavelength slots. *IEEE Antennas and Wireless Propagation Letters, 11*, 411–414.
19. Kim, D. O., Jo, N. I., Choi, D. M., & Kim, C.-Y. (2009). Design of the ultra-wideband antenna with 5.2 GHz/5.8 GHz band rejection using rectangular split-ring resonators (SRRs) loading. *Journal of Electromagnetic Waves and Applications, 23*(17–18), 2503–2512.
20. Baena, J. D., Bonache, J., Martin, F., Sillero, R. M., Falcone, F., Lopetegi, T., et al. (2005). Equivalent-circuit models for split ring resonators and complementary split-ring resonators coupled to planar transmission lines. *IEEE Transactions on Microwave Theory Techniques, 53*, 1451–1461.
21. Bonache, J., Gil, M., García-García, J., & Martín, F. (2006). On the electrical characteristics of complementary metamaterial resonators. *IEEE Microwave and Wireless Components Letters, 16*, 543–545.

Manas Sarkar was born in West Bengal, India. He received his B.Tech degree in Radio Physics and Electronics from University of Calcutta, Kolkata in the year of 2002 and M.E. degree from Jadavpur in the year 2004. Presently he is working as an engineer in Indian Space Research Organization (ISRO). At the same time he is pursuing Ph.D. from Indian School of Mines, Dhanbad, also. His research interest includes Feed design, Antennas, Radome and RF circuits.

Santanu Dwari was born in Howrah, West Bengal, India. He received his B.Tech and M.Tech degree in Radio Physics and Electronics from University of Calcutta, Kolkata, West Bengal, India in the year of 2000 and 2002 respectively and Ph.D. degree from Indian Institute of Technology, Kharagpur, West Bengal, India in the year of 2009. He joined Indian School of Mines, Dhanbad, Jharkhand, India in 2008 where he is currently an Assistant Professor in the Department of Electronics Engineering. He has published several research papers in referred International Journals. He is carrying out two sponsored research project as Principal Investigator. His research interest includes Antennas, RF planar circuits, Computational Electromagnetics.

Anitha Daniel received her B.E.(Hons) in ECE from Madurai Kamraj University, India in 1987 and M.E. in ECE from I.I.S.C. Bangalore, India in 1996. Since 1988 has been working in Radar Development Area, Indian Space Research Organization and has contributed to the development of RF Subsystems of Doppler Weather Radars & Atmospheric Radars.